Structural Engineering and Mechanics, *Vol. 75, No. 2 (2020) 193-209*
DOI: https://doi.org/10.12989/sem.2020.75.2.193

A novel hyperbolic plate theory including stretching effect for free vibration analysis of advanced composite plates in thermal environments

Setti Elmascri[1,3], Aicha Bessaim*[2], Ouahiba Taleb[2], Mohammed Sid Ahmed Houari[2], Sekkal Mohamed[3], Fabrice Bernard[4] and Abdelouahed Tounsi[3,5]

[1]*Department of Civil Engineering, University Abdelhamid Ibn Badis of Mostaganem, Algeria*
[2]*Laboratoire d'Etude des Structures et de Mécanique des Matériaux, Département de Génie Civil, Faculté des Sciences et de la Technologie, Université Mustapha Stambouli, Mascara, Algeria*
[3]*Material and Hydrology Laboratory, University of Sidi Bel Abbes, Faculty of Technology, Civil Engineering Department, Algeria*
[4]*Université Européenne de Bretagne, INSA Rennes, LGCGM, 20 avenue des Buttes de coësmes 35708 Rennes Cedex 7, France*
[5]*Department of Civil and Environmental Engineering, King Fahd University of Petroleum and Minerals, 31261 Dhahran, Eastern Province, Saudi Arabia*

(Received September 26, 2019, Revised December 18, 2019, Accepted February 17, 2020)

Abstract. This paper presents a new hyperbolic shear deformation plate theory including the stretching effect for free vibration of the simply supported functionally graded plates in thermal environments. The theory accounts for parabolic distribution of the transverse shear strains and satisfies the zero traction boundary conditions on the surfaces of the plate without using shear correction factors. This theory has only five unknowns, which is even less than the other shear and normal deformation theories. The present one has a new displacement field which introduces undetermined integral variables. Material properties are assumed to be temperature-dependent, and graded in the thickness direction according to a simple power law distribution in terms of the volume power laws of the constituents. The equation of motion of the vibrated plate obtained via the classical Hamilton's principle and solved using Navier's steps. The accuracy of the proposed solution is checked by comparing the present results with those available in existing literature. The effects of the temperature field, volume fraction index of functionally graded material, side-to-thickness ratio on free vibration responses of the functionally graded plates are investigated. It can be concluded that the present theory is not only accurate but also simple in predicting the natural frequencies of functionally graded plates with stretching effect in thermal environments.

Keywords: Functionally Graded (FG) plates; vibration; new plate theory; shear and normal deformation, analytical modeling, thermal environment

1. Introduction

Functionally graded materials (FGMs) are a novel class of composites increasingly used in many fields of engineering fields, especially in high temperature applications such as thermo-mechanical loadings structures, aircraft, spacecraft, plasma coatings for fusion reactors and other engineering structures under high-temperature environment (Li *et al*. 2008, Kar and Panda, 2015, Taleb *et al*. 2018, Tu *et al*. 2019), the important advantages offered by functionally graded materials over conventional composite materials are eliminated the interface problems of conventional composite materials and the stress distribution becomes mitigated (Taleb *et al*. 2018). This can be obtained by gradually varying the volume fraction of constituent materials, their material properties show a smooth and continuous change from one surface to another. Typically FGM is made of ceramic and metal, the ceramic constituent provides the high-temperature resistance due to its low thermal conductivity, while the ductile metal constituent prevents fracture due to its toughness, thus are being capable to withstand intense high temperature gradient while preserve structural integrity (Tu *et al*. 2019, Huang and Shen 2004). Functionally graded materials were in first time designed as thermal barrier materials for fusion reactors and aerospace structures where extremely high temperature and large thermal gradient exist (Ebrahimi, 2013). Thus, thermal response of these structures have been receiving considerably attention. Nowadays, functionally graded materials are employed in wide engineering applications including nuclear, mechanical and civil engineering. Hence, examining their responses under various types of loading using accurate models of structures (plates, beams and shell) is extremely important. Subsequently, many studies on analysis of bending, vibration, thermomechanical and buckling behaviors of functionally graded structural members have been performed in recent years by many researchers (Ebrahimi and Jafari,2016, Kar and Panda, 2014, Kolahchi *et al*. 2015, Darilmaz *et al*. 2015, Darilmaz, 2015, Pandey and Pradyumna, 2015, Khalili and Mohammadi, 2012, Yaghoobi and Yaghoobi, 2013, Alibeigloo and Alizadeh, 2015, Fazzolari, 2016, Mehar and Panda, 2018, Lashkari and Rahmani, 2016, Van Long *et al*. 2016, Akbaş, 2017,

*Corresponding author, Ph.D.
E-mail: a.bessaim@univ-mascara.dz; bessaimaicha@yahoo.fr

ISSN: 1225-4568 (Print), 1598-6217 (Online)

Adhikari and Singh, 2019, Tornabene, 2009, Neves *et al*. 2019, Carrera *et al*. 2011, El Meiche *et al*. 2011, Zenkour and Sobhy, 2010, Zarga *et al*. 2019, Karami *et al*. 2019), and an extensive range of plate theories have been developed to provide more correctly their mechanical responses. These plate theories can be divided into three groups namely: classical plate theory (CPT), first-order shear deformation plate theory (FSDT) and higher-order shear deformation plate theory (HSDT). The Classical plate theory (CPT), which neglects the transverse shear deformation effect, gives a reasonable results only for the analysis of thin plates without transverse shear deformation effect. However, the first-order shear deformation plate theory (FSDT) surmounts this problem by taking into account this effect, is appropriate for both thin and moderately thick plates. Nevertheless, an appropriate shear correction factor is needed to correct the transverse shear stress distribution. In order to avoid using shear correction factors, the higher-order shear deformation theories (HSDTs) have been developed which are either based on the three-dimensional approach or the two dimensional approach with a nonlinear variation of high order axial displacement giving parabolic variation of transverse shear strains through the plate thickness (Kant, 1993). Therefore, this theory has been more and more used to predict the behavior of functionally graded plates by giving the possibility to increase the accuracy of numerical evaluations for moderately thick plates and very thick plates (Kant and Swaminathan, 2001). A significant number of articles about the free vibrations of functionally graded plates in thermal environment have been performed using various plate theories. Chakraverty and Pradhan (2014) have used the classical plate theory to investigate the free vibration of functionally graded plate in thermal environment subject to various sets of boundary conditions. Wang and Zu (2017) studied the free vibrations of FG rectangular plates with porosities and moving in thermal environment by using von Kármán nonlinear plate theory. Parida and Mohanty (2018) investigated free vibration behavior of FG skew plates using higher-order shear deformation plate theory (HSDT) under thermal environment. Yang *et al*. (2003) developed a semi-analytical approach in terms of one-dimensional differential quadrature and Galerkin technique to analyze the large amplitude vibration of initially stressed FGM laminated rectangular plates with thermo-electromechanical loading. Kim (2005) developed a method to analyze the effect of temperature on the vibration behaviour of the functionally graded pre-stressed plate. Huang and Shen (2004) applied the perturbation technique to studied the nonlinear vibration and dynamic response of functionally graded material plates by taking into account heat conduction and temperature-dependent material properties. Li *et al*. (2008) studied the free vibration of rectangular FGM plate in thermal environment with simply supported and clamp boundary conditions using the three dimensional elasticity theory in which displacements are expressed by a series of Chebyshev polynomial multiplied by appropriate functions. Joshi *et al*. (2016) studied the buckling and free vibration of partially cracked thin orthotropic rectangular plates in thermal environment. Cui and Hu (2016) studied the natural vibration and thermal buckling of uniformly heated rectangular thin plates with stick-slip-stop boundaries. Pandey and Pradyumna (2015) carried out the free vibration analysis of the sandwich plates with functionally graded material face-sheets and the sandwich plates with functionally graded material core using the layerwise finite element formulation under nonlinear temperature distribution through the thickness. Daikh (2019) presented an exact solution of nonlinear temperature distribution for free vibration of simply supported functionally graded sandwich plates resting on elastic foundation. Free and forced vibration responses of functionally graded plates under high temperature loading was investigated by Wattanasakulpong *et al*. (2013) applying the improved third-order shear deformation plate theory. Using the eight-unknown higher order shear deformation plate theory, Tran *et al*. (2019) investigated free vibration responses of functionally graded plates subjected to thermal loads.

The novelty of this paper is the use of recently developed polynomial and nonpolynomial based higher-order shear deformation theories presented by Tounsi and his co-workers (Karami *et al*. 2018ab, Zaoui *et al*. 2019, Medani *et al*. 2019, Mahmoudi *et al*. 2019) by including the so-called stretching effect to investigate the free vibration analysis of graded plates in thermal environment including the stretching effect. It should be noted that the thickness stretching effect is ignored in these new four variable plate theories and the transverse displacement is considered constant in the thickness direction, as in Kirchhoff–Love type thin plate theories. This appears quite inadequate since FGM plates are characterized by a strong variation of material properties in the thickness direction. The most interesting feature of this theory is that it accounts for a hyperbolic variation of the transverse shear strains across the thickness and satisfies the zero traction boundary conditions on the top and bottom surfaces of the plate without using shear correction factors. It should be noted that the hyperbolic function was used in the first time by Nguyen (2015) and Taleb *et al*. (2018). Using the proposed theory, both free vibration analysis of FG plates in thermal environment are investigated. Three types of environmental condition namely uniform, linear and nonlinear thermal load are imposed at the upper and lower surface for simply supported FG plates. Material properties are assumed to be temperature-dependent, and vary continuously with the thickness according to a power law distribution in terms of the volume power laws of the constituents. In this study, analytical of vibration solutions are obtained for functionally graded plate and accuracy is verified by comparing the obtained results with those reported in the literature. The influences of some parameters including gradient index, plate geometry, mode number and thermal loading on the vibration characteristics of the FG plates are presented. It can be concluded that the present theories are not only accurate but also simple in predicting the free vibration responses of temperature-dependent FG plates.

2. Theoretical formulation

2.1. Power-law FG plate equations based

Consider a simply supported rectangular functionally graded plate of length a, width b and uniform thickness h in the unstressed reference configuration. The coordinate system for FG plates is shown in Fig. 1.

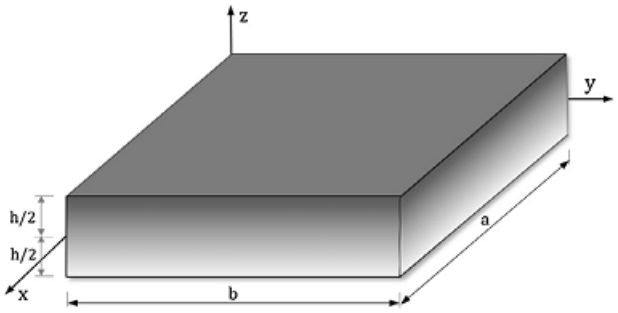

Fig. 1 Geometry of rectangular FGM plate with uniform thickness in the rectangular cartesian coordinates

The FG plate is made of elastic and isotropic functionally graded material with its material properties vary smoothly through the thickness direction only. The effective material properties of the FG plate such as Young's modulus $E(z)$, thermal conductivity $k(z)$, thermal expansion $\alpha(z)$ and mass density $\rho(z)$ based on the rule of mixture, and are expressed as (Bourada *et al*. 2019, Berghouti *et al*. 2019):

$$P_{eff}(z) = P_m + (P_c - P_m)\left(\frac{z}{h} + \frac{1}{2}\right)^p \tag{1}$$

To predict the behavior of FGMs under high temperature more precisely, it is needful to consider the temperature dependency on material properties. The nonlinear equation of thermo-elastic material properties in function of temperature $T(K)$ can be expressed as the following (Shahrjerdi *et al*. 2011, Attia *et al*. 2015):

$$P(z) = P_0\left(P_{-1}T^{-1} + 1 + P_1T + P_2T^2 + P_3T^3\right) \tag{2}$$

where $P(z)$ denotes material property and $T=T_0+\Delta T(z)$ indicates the environmental temperature, $T_0=300(K)$ is room temperature, P_{-1}, P_0, P_1, P_2 and P_3 are the coefficients of temperature dependent material properties unique to the constituent materials which can be seen in the table of materials properties (Table 1) for FG (ZrO_2/Ti-6Al-4V) and (Si_3N_4/ SUS304), and $\Delta T(z)$ is the temperature rise only through the thickness direction, whereas thermal conductivity k is temperature-independent.

2.2 Constitutive equations

For elastic and isotropic FGMs, the linear constitutive relations can be written as:

$$\begin{Bmatrix}\sigma_x\\ \sigma_y\\ \sigma_z\\ \tau_{yz}\\ \tau_{xz}\\ \tau_{xy}\end{Bmatrix} = \begin{bmatrix}Q_{11} & Q_{12} & Q_{13} & 0 & 0 & 0\\ Q_{12} & Q_{22} & Q_{23} & 0 & 0 & 0\\ Q_{13} & Q_{23} & Q_{33} & 0 & 0 & 0\\ 0 & 0 & 0 & Q_{44} & 0 & 0\\ 0 & 0 & 0 & 0 & Q_{55} & 0\\ 0 & 0 & 0 & 0 & 0 & Q_{66}\end{bmatrix}\begin{Bmatrix}\varepsilon_x\\ \varepsilon_y\\ \varepsilon_z\\ \gamma_{yz}\\ \gamma_{xz}\\ \gamma_{xy}\end{Bmatrix} \tag{3}$$

where $(\sigma_x,\sigma_y,\sigma_z,\tau_{yz},\tau_{xz},\tau_{xy})$ and $(\varepsilon_x,\varepsilon_y,\varepsilon_z,\gamma_{yz},\gamma_{xz},\gamma_{xy})$ are stress and strain components, respectively.

The computation of the elastic constants Q_{ij} depends on which assumption of ε_z are considered. Using the material properties defined in Eq. (1), stiffness coefficients, Q_{ij}, can be expressed as

$$Q_{11} = Q_{22} = Q_{33} = \frac{(1-\nu)E(z,T)}{(1-2\nu)(1+\nu)}, \tag{4a}$$

$$Q_{12} = Q_{13} = Q_{23} = \frac{\nu\,E(z,T)}{(1-2\nu)(1+\nu)}, \tag{4b}$$

$$Q_{44} = Q_{55} = Q_{66} = \frac{E(z,T)}{2(1+\nu)}, \tag{4c}$$

Note that for higher-order shear deformation theory (HSDT) which neglect the thickness stretching $\varepsilon_z = 0$, the coefficients Q_{ij} should be:

$$Q_{11} = Q_{22} = \frac{E(z,T)}{1-\nu^2}, \tag{5a}$$

$$Q_{12} = \nu\,Q_{11}, \tag{5b}$$

$$Q_{12} = Q_{13} = Q_{23} = \frac{\nu\,E(z,T)}{(1-2\nu)(1+\nu)}, \tag{5c}$$

Based on the thick plate theory and including the effect of transverse normal stress (thickness stretching effect), the basic assumptions for the displacement field of the plate can be described as

$$u(x,y,z,t) = u_0(x,y,t) - z\frac{\partial w_0}{\partial x} + k_1\,f(z)\int\theta(x,y,t)\,dx \tag{6a}$$

$$v(x,y,z,t) = v_0(x,y,t) - z\frac{\partial w_0}{\partial y} + k_2\,f(z)\int\theta(x,y,t)\,dy \tag{6b}$$

$$w(x,y,z,t) = w_0(x,y,t) + g(z)\varphi_z(x,y,t) \tag{6c}$$

The coefficients k_1 and k_2 depends on the geometry and the proposed theory of present study has a hyperbolic function in the form (Taleb *et al*. 2018, Nguyen 2015)

$$f(z) = \sinh^{-1}\left(\frac{3z}{h}\right) - z\frac{6}{h\sqrt{13}} \tag{7}$$

It can be observed that the kinematic in Eq. (6) uses only five unknowns (u_0, v_0, w_0, θ and φ_z). Nonzero strains of the five variable plate model are expressed as follows:

$$\begin{Bmatrix}\varepsilon_x\\ \varepsilon_y\\ \gamma_{xy}\end{Bmatrix} = \begin{Bmatrix}\varepsilon_x^0\\ \varepsilon_y^0\\ \gamma_{xy}^0\end{Bmatrix} + z\begin{Bmatrix}k_x^b\\ k_y^b\\ k_{xy}^b\end{Bmatrix} + f(z)\begin{Bmatrix}k_x^s\\ k_y^s\\ k_{xy}^s\end{Bmatrix}, \tag{8a}$$

$$\begin{Bmatrix}\gamma_{yz}\\ \gamma_{xz}\end{Bmatrix} = g(z)\begin{Bmatrix}\gamma_{yz}^0\\ \gamma_{xz}^0\end{Bmatrix}, \tag{8b}$$

Table 1 Temperature-dependent material properties for (ZrO_2/Ti-6Al-4V) and (Si_3N_4/ SUS304)

Material	Properties	P_0	P_{-1}	P_1	P_2	P_3
Si_3N_4	E(GPa)	348.43	0	-3.070 × 10^{-4}	2.160 × 10^{-7}	-8.946 × 10^{-11}
	α(K^{-1})	5.8723 × 10^{-6}	0	9.095 × 10^{-6}	0	0
	ρ(Kg/m^3)	2370	0	0	0	0
	ν	0.24	0	0	0	0
	k	9.19	0	0	0	0
SUS304	E(GPa)	201.04	0	3.079 × 10^{-4}	-6.534 × 10^{-7}	0
	α(K^{-1})	12.330 × 10^{-6}	0	8.086 × 10^{-4}	0	0
	ρ(Kg/m^3)	8166	0	0	0	0
	ν	0.3262	0	-2.002 × 10^{-4}	3.797 × 10^{-7}	0
	k	12.04	0	0	0	0
ZrO_2	E(GPa)	244.27	0	-1.371 × 10^{-3}	1.214 × 10^{-6}	-3.681 × 10^{-10}
	α(K^{-1})	12.766 × 10^{-6}	0	-1.491 × 10^{-3}	1.006 × 10^{-5}	-6.788 × 10^{-11}
	ρ(Kg/m^3)	3000	0	0	0	0
	ν	0.3330	0	0	0	0
	k	1.80	0	0	0	0
Ti-6Al-4V	E(GPa)	122.56	0	-4.586 × 10^{-4}	0	0
	α(K^{-1})	7.75788 × 10^{-6}	0	6.638 × 10^{-4}	-3.147 × 10^{-6}	0
	ρ(Kg/m^3)	4429	0	0	0	0
	ν	0.2888	0	1.108 × 10^{-4}	0	0
	k	7.82	0	0	0	0

$$\varepsilon_z = g'(z)\,\varepsilon_z^0 \tag{8c}$$

where

$$\begin{Bmatrix} \varepsilon_x^0 \\ \varepsilon_y^0 \\ \gamma_{xy}^0 \end{Bmatrix} = \begin{Bmatrix} \dfrac{\partial u_0}{\partial x} \\ \dfrac{\partial v_0}{\partial x} \\ \dfrac{\partial u_0}{\partial y} + \dfrac{\partial v_0}{\partial x} \end{Bmatrix}, \tag{9a}$$

$$\begin{Bmatrix} k_x^b \\ k_y^b \\ k_{xy}^b \end{Bmatrix} = \begin{Bmatrix} -\dfrac{\partial^2 w_0}{\partial x^2} \\ -\dfrac{\partial^2 w_0}{\partial y^2} \\ -2\dfrac{\partial^2 w_0}{\partial x \partial y} \end{Bmatrix}, \tag{9b}$$

$$\begin{Bmatrix} k_x^s \\ k_y^s \\ k_{xy}^s \end{Bmatrix} = \begin{Bmatrix} k_1\theta \\ k_2\theta \\ k_1\dfrac{\partial}{\partial y}\int \theta\, dx + k_2\dfrac{\partial}{\partial x}\int \theta\, dy \end{Bmatrix} \tag{9c}$$

$$\begin{Bmatrix} \gamma_{yz}^0 \\ \gamma_{xz}^0 \end{Bmatrix} = \begin{Bmatrix} k_2\int \theta\, dy + \dfrac{\partial \varphi_z}{\partial y} \\ k_1\int \theta\, dx + \dfrac{\partial \varphi_z}{\partial x} \end{Bmatrix} \tag{9d}$$

and

$$\varepsilon_z^0 = \varphi_z, \qquad g'(z) = \frac{dg(z)}{dz} \tag{9e}$$

It can be observed from equation (7) that the transverse shear strains (γ_{xz}, γ_{yx}) are equal to zero at the upper (z= h/2) and lower (z= -h/2) surfaces of the plate. A shear correction coefficient is, hence, not required. The integrals used in the above equations shall be resolved by a Navier type procedure and can be expressed as follows (Taleb *et al*. 2018):

$$\frac{\partial}{\partial y}\int \theta\, dx = A'\frac{\partial^2 \theta}{\partial x \partial y}, \quad \frac{\partial}{\partial x}\int \theta\, dy = B'\frac{\partial^2 \theta}{\partial x \partial y}, \quad \int \theta\, dx = A'\frac{\partial \theta}{\partial x}, \quad \int \theta\, dy = B'\frac{\partial \theta}{\partial y} \tag{10}$$

where the coefficients A' and B' are considered according to the type of solution employed, in this case via Navier method. Therefore, A', B', k_1 and k_2 are expressed as follows:

$$A'=-\frac{1}{\alpha^2},\quad B'=-\frac{1}{\beta^2},\quad k_1=\alpha^2,\quad k_2=\beta^2 \tag{11}$$

where α, and β are defined in equation (33).

2.3 Governing equations

The equations of motion for the free vibration of the functionally graded plates can be derived from the Hamilton's principle:

$$\int_{t_1}^{t_2}\left(\delta K-\delta U\right)dt=0 \tag{12}$$

where t is the time, t_1 and t_2 are the initial and end times, respectively, δK is the variation of the kinetic energy and δU is the variation of the total strain energy. The total strain energy of the beam can be represented as:

$$U=U_d+U_T \tag{13}$$

where U_d is the strain energy due to the mechanical stresses and U_T is the strain energy caused by the initial stresses due to temperature rise. The strain energy U_d and U_T are given by (Li *et al*. 2008, Kim, 2005, Shahrjerdi *et al*. 2011):

$$U_d=\int_V\left(\sigma_x\delta\varepsilon_x+\sigma_y\delta\varepsilon_y+\sigma_z\delta\varepsilon_z+\tau_{xy}\delta\gamma_{xy}+\tau_{yz}\delta\gamma_{yz}+\tau_{xz}\delta\gamma_{xz}\right)dAdz \tag{14a}$$

$$U_T=\frac{1}{2}\int_V\left[\sigma_x^T\,d_{11}+\sigma_y^T\,d_{22}\right]dV \tag{14b}$$

where d_{ij}, (i,j =1,2) is the nonlinear strain-displacement relationship (Shahrjerdi *et al*. 2011). By substituting d_{ij} into Eq. (14) the following equation is obtained:

$$U_T=\frac{1}{2}\int_V\left[\sigma_x^T\left[\left(\frac{\partial^2u}{\partial x^2}+\frac{\partial^2v}{\partial x^2}+\frac{\partial^2w}{\partial x^2}\right)\right]+\sigma_y^T\left[\left(\frac{\partial^2u}{\partial y^2}+\frac{\partial^2v}{\partial y^2}+\frac{\partial^2w}{\partial y^2}\right)\right]\right]dV \tag{15}$$

In Eq. (15), the thermal stresses σ_x^T and σ_y^T are given by (Attia *et al*. 2015, Daikh, 2019):

$$\sigma_x^T=-\left(Q_{11}+Q_{12}\right)\alpha\left(z,T\right)\Delta T\left(z\right) \tag{16a}$$

$$\sigma_y^T=-\left(Q_{21}+Q_{22}\right)\alpha\left(z,T\right)\Delta T\left(z\right) \tag{16b}$$

The kinetic energy of plate can be expressed as:

$$K=\frac{1}{2}\int_V\rho\left(z,T\right)\left(\dot{u}+\dot{v}+\dot{w}\right)dV \tag{17}$$

By substituting eqs. (13)-(17), into Eq. (12) and integrating by parts with respect to space and time variables, the equations of motion in terms of the displacement components of the FG plate are obtained as

$$\begin{aligned}&\left(A_{11}+A_{11}^T\right)d_{11}u_0+\left(A_{66}+A_{22}^T\right)d_{22}u_0+\left(A_{12}+A_{66}\right)d_{12}v_0\\&-\left(B_{11}+B_{11}^T\right)d_{111}w_0-\left(B_{12}+2B_{66}+B_{22}^T\right)d_{122}w_0\\&+\left(B_{66}^s\left(k_1A^{'}+k_2\,B^{'}\right)+B_{12}^sk_2B^{'}+B_{22}^{sT}\,k_1A^{'}\right)d_{122}\theta\\&+\left(B_{11}^s+B_{11}^{sT}\right)k_1A^{'}\,d_{111}\theta+L\,d_1\varphi_z=I_0\ddot{u}_0-I_1d_1\ddot{w}_0\\&+k_1A^{'}\,J_1d_1\ddot{\theta},\end{aligned} \tag{18a}$$

$$\begin{aligned}&\left(A_{22}+A_{22}^T\right)d_{22}v_0+\left(A_{66}+A_{11}^T\right)d_{11}v_0+\left(A_{12}+A_{66}\right)d_{12}u_0\\&-\left(B_{22}+B_{22}^T\right)d_{222}w_0\\&-\left(B_{12}+2B_{66}+B_{11}^T\right)d_{112}w_0\\&+\left(B_{66}^s\left(k_1A^{'}+k_2\,B^{'}\right)+B_{12}^sk_1A^{'}+B_{11}^{sT}\,k_2B^{'}\right)d_{112}\theta\\&+\left(B_{22}^s+B_{22}^{sT}\right)k_2B^{'}\,d_{222}\theta+L\,d_1\varphi_z=I_0\ddot{v}_0-I_1\,d_2\ddot{w}_0\\&+k_2B^{'}J_1\;d_2\ddot{\theta},\end{aligned} \tag{18b}$$

$$\begin{aligned}&\left(B_{11}+B_{11}^T\right)d_{111}u_0+\left(B_{12}+2B_{66}+B_{22}^T\right)d_{122}u_0\\&+\left(B_{12}+2B_{66}+B_{11}^T\right)d_{112}v_0+\left(B_{22}+B_{22}^T\right)d_{222}v_0\\&-\left(D_{11}+D_{11}^T\right)d_{1111}w_0-2\left(D_{12}+2D_{66}\right)d_{1122}w_0\\&-\left(D_{22}+D_{22}^T\right)d_{2222}w_0+\left(D_{11}^s+D_{11}^{sT}\right)k_1A^{'}d_{1111}\theta\\&+\left(\left(D_{12}^s+2D_{66}^s\right)\left(k_1A^{'}+k_2B^{'}\right)\right)d_{1122}\theta+\left(D_{22}^s+D_{22}^{sT}\right)k_2\,B^{'}d_{2222}\theta\\&+\left(D_{11}^{sT}k_2\,B^{'}+D_{22}^{sT}k_1\,A^{'}\right)d_{1122}\theta\\&-\left(D_{11}^T+D_{22}^T\right)d_{1122}w_0+A_{11}^Td_{11}w_0+A_{22}^Td_{11}w_0\\&+\left(L^s+E_{11}^T\right)d_{11}\varphi_z+\left(L^s+E_{22}^T\right)d_{22}\varphi_z=I_0\ddot{w}_0+\\&I_1\left(d_1\ddot{u}_0+d_2\,\ddot{v}_0\right)-I_2\left(d_{11}\ddot{w}_0+d_{22}\ddot{w}_0\right)\\&+J_2\left(k_1A^{'}\,d_{11}\ddot{\theta}+k_2\,B^{'}\,d_{22}\ddot{\theta}\right)+J_0\ddot{\varphi}_z\end{aligned} \tag{18c}$$

$$\begin{aligned}&-\left(B_{11}^s+B_{11}^{sT}\right)k_1A^{'}d_{111}u_0\\&-\left(B_{12}^sk_2B^{'}+B_{22}^{sT}k_1A^{'}+B_{66}^s\left(k_1A^{'}+k_2B^{'}\right)\right)d_{122}u_0\\&-\left(B_{12}^sk_1A^{'}+B_{11}^{sT}k_2B^{'}+B_{66}^s\left(k_1A^{'}+k_2B^{'}\right)\right)d_{112}v_0\\&-\left(B_{22}^s+B_{22}^{sT}\right)k_2B^{'}d_{222}v_0\\&+\left(D_{11}^s+D_{11}^{sT}\right)k_1A^{'}d_{1111}w_0\\&+\left(\left(D_{12}^s+2D_{66}^s\right)\left(k_1A^{'}+k_2B^{'}\right)\right)d_{1122}w_0\\&+\left(D_{22}^s+D_{22}^{sT}\right)k_2B^{'}d_{2222}w_0\\&-\left(H_{11}^s+H_{11}^{sT}\right)\left(k_1A^{'}\right)^2d_{1111}\theta-\left(H_{22}^s+H_{22}^{sT}\right)\left(k_2B^{'}\right)^2d_{2222}\theta\\&-\left(2H_{12}^sk_1k_2A^{'}B^{'}+\left(k_1A^{'}+k_2B^{'}\right)^2H_{66}^s\right)d_{1122}\theta\\&+A_{44}^s\left(k_2B^{'}\right)^2d_{22}\theta+A_{55}^s\left(k_1\,A^{'}\right)^2d_{11}\theta\\&+\left(D_{11}^{sT}k_2\,B^{'}+D_{22}^{sT}k_1\,A^{'}\right)d_{1122}w_0\\&-\left(H_{11}^{sT}\left(k_2\,B^{'}\right)^2+H_{22}^{sT}\left(k_1\,A^{'}\right)^2\right)d_{1122}\theta\\&+k_1A^{'}\left(R-A_{55}^s\right)d_{11}\varphi_z\\&+k_2B^{'}\left(R-A_{44}^s\right)d_{22}\varphi_z=-J_1\left(k_1\,A^{'}d_1\ddot{u}_0+k_2\,B^{'}\,d_2\ddot{v}_0\right)\\&+J_2\left(k_1\,A^{'}d_{11}\ddot{w}_0+k_2\,B^{'}\,d_{22}\ddot{w}_0\right)\\&-K_2\left(\left(k_1A^{'}\right)^2d_{11}\ddot{\theta}+\left(k_2\,B^{'}\right)^2d_{22}\ddot{\theta}\right)\end{aligned} \tag{18d}$$

$$\begin{aligned}&Ld_1u_0+Ld_2v_0-\left(L^s+E_{11}^T\right)d_{11}w_0-\left(L^s+E_{22}^T\right)d_{22}w_0\\&+k_1A^{'}\left(L^s-A_{55}^s\right)d_{11}\theta+k_2B^{'}\left(L^s-A_{44}^s\right)d_{22}\theta\\&-\left(A_{55}^s+F_{11}^T\right)d_{11}\varphi_z-\left(A_{44}^s+F_{22}^T\right)d_{22}\varphi_z+R^s\varphi_z=J_0\ddot{w}+K_3\ddot{\varphi}_z\end{aligned} \tag{18e}$$

where d_{ij}, d_{ijl} and d_{ijm} are the following differential operators:

$$d_{ij}=\frac{\partial^2}{\partial x_i\partial x_j},\quad d_{ijl}=\frac{\partial^3}{\partial x_i\partial x_j\partial x_l},\quad d_{ijlm}=\frac{\partial^4}{\partial x_i\partial x_j\partial x_l\partial x_m},\quad d_i=\frac{\partial}{\partial x_i},\quad (i,j,l,m=1,2). \tag{19}$$

and stiffness components are calculated as:

$$\left\{\begin{matrix}A_{11},B_{11},D_{11},B_{11}^s,D_{11}^s,H_{11}^s\\A_{12},B_{12},D_{12},B_{12}^s,D_{12}^s,H_{12}^s\\A_{66},B_{66},D_{66},B_{66}^s,D_{66}^s,H_{66}^s\end{matrix}\right\}= \int_{-h/2}^{h/2}Q_{11}\left(1,z,z^2,f(z),z\,f(z),f^2(z)\right)\left\{\begin{matrix}1\\\nu\\\frac{1-\nu}{2}\end{matrix}\right\}dz \tag{20}$$

$$\left(A_{22},B_{22},D_{22},B_{22}^s,D_{22}^s,H_{22}^s\right)=\left(A_{11},B_{11},D_{11},B_{11}^s,D_{11}^s,H_{11}^s\right) \tag{21}$$

$$A_{44}^s=A_{55}^s\int_{-h/2}^{h/2}Q_{44}\left[g^2(z)\right]dz \tag{22}$$

$$\left(L,L^s,R,R^s\right)=\int_{-h/2}^{h/2}\left(1,z,f(z),g'(z)\right)g'(z)Q_{13}dz \tag{23}$$

$$\left\{\begin{matrix}A_{11}^T,B_{11}^T,D_{11}^T,B_{11}^{sT},D_{11}^{sT},H_{11}^{sT},E_{11}^T,F_{11}^T\\A_{22}^T,B_{22}^T,D_{22}^T,B_{22}^{sT},D_{22}^{sT},H_{22}^{sT},E_{22}^T,F_{22}^T\end{matrix}\right\}= \int_{-h/2}^{h/2}\left(1,z,z^2,f(z),z\,f(z),f^2(z),g(z),g(z)^2\right)\left\{\begin{matrix}\sigma_x^T\\\sigma_y^T\end{matrix}\right\}dz \tag{24}$$

The inertias are also defined as

$$\left(I_0,J_0,I_1,I_2\right)=\int_{-h/2}^{h/2}\left(1,g(z),z,z^2\right)\rho(z)dz \tag{25a}$$

$$\left(J_1,J_2,K_2,K_3\right)=\int_{-h/2}^{h/2}\left(f(z),z\,f(z),f^2(z),g^2(z)\right)\rho(z)dz \tag{25b}$$

2.4 Temperature field

In this study, four cases of one-dimensional temperature distribution through the thickness are considered, with $T=T(z)$.

2.4.1 Uniform temperature

In this case, a uniform temperature field is used as follows

$$T(z)=T_0+\Delta T(z) \tag{26}$$

where $\Delta T(z)$ denotes the temperature change and T_0=300K is room temperature.

2.4.2 Linear temperature

For a functionally graded plate, assuming temperatures T_b and T_t are imposed at the bottom and top of the plate, the temperature field under linear temperature rise along the thickness can be obtained as follows:

$$T(z)=T_0+\Delta T\left(\frac{z}{h}+\frac{1}{2}\right) \tag{27}$$

2.4.3 Nonlinear temperature

The nonlinear temperature rise across the thickness of the plate is determined by solving the one dimensional heat conduction equation. The one dimensional steady-state heat conduction equation in the z-direction is given by:

$$T(z)=-\frac{d}{dz}\left(k(z)\frac{dT}{dz}\right) \tag{28}$$

with the boundary condition $T(h/2)=T_t$ and $T(-h/2)=T_b=T_0$. Here a stress-free state is assumed to exist at T_0=300K. The thermal conductivity coefficient $k(z)$ is assumed here to obey the power-law relation in Eq. (1). The analytical solution to Eq. (28) is

$$T(z)=T_b-\left(T_t-T_b\right)\frac{\int_{-h/2}^{z}\frac{1}{k(z)}dz}{\int_{-h/2}^{h/2}\frac{1}{k(z)}dz} \tag{29}$$

In the case of power-law FG plate, the solution of Eq. (16) also can be expressed by means of a polynomial series (Shahrjerdi *et al*. 2011, Attia *et al*. 2015):

$$T(z)=T_b+\frac{(T_t-T_b)}{C_{tb}}\left[\left(\frac{2z+h}{2h}\right)-\frac{k_{tb}}{(p+1)k_b}\left(\frac{2z+h}{2h}\right)^{p+1}+\frac{k_{tb}^2}{(2p+1)k_b^2}\left(\frac{2z+h}{2h}\right)^{2p+1}-\frac{k_{tb}^3}{(4p+1)k_b^3}\left(\frac{2z+h}{2h}\right)^{3p+1}+\frac{k_{tb}^4}{(4p+1)k_b^4}\left(\frac{2z+h}{2h}\right)^{4p+1}-\frac{k_{tb}^5}{(5p+1)k_b^5}\left(\frac{2z+h}{2h}\right)^{5p+1}\right] \tag{30}$$

with

$$C_{tb}=1-\frac{k_{tb}}{(p+1)k_b}+\frac{k_{tb}^2}{(2p+1)k_b^2}+\frac{k_{tb}^3}{(3p+1)k_b^3}+\frac{k_{tb}^4}{(4p+1)k_b^4}+\frac{k_{tb}^5}{(5p+1)k_b^5} \tag{31}$$

where $k_{tb}=k_t-k_b$, with k_t and k_b are the thermal conductivity of the top and bottom faces of the plate, respectively.

3. Analytical Solution of Simply Supported FG plate

In this work, we are concerned with the exact solutions of equation (18) for a simply supported nanoplate. Using the Navier solution procedure, the following expressions of displacements (u_0, v_0, w_0, θ, and φ_z) are taken:

$$\left\{\begin{matrix}u_0\\v_0\\w_0\\\theta\\\varphi_z\end{matrix}\right\}=\left\{\begin{matrix}U_{mn}e^{i\omega t}\cos(\alpha x)\sin(\beta y)\\V_{mn}e^{i\omega t}\sin(\alpha x)\cos(\beta y)\\W_{mn}e^{i\omega t}\sin(\alpha x)\sin(\beta y)\\X_{mn}e^{i\omega t}\sin(\alpha x)\sin(\beta y)\\Z_{mn}e^{i\omega t}\sin(\alpha x)\sin(\beta y)\end{matrix}\right\} \tag{32}$$

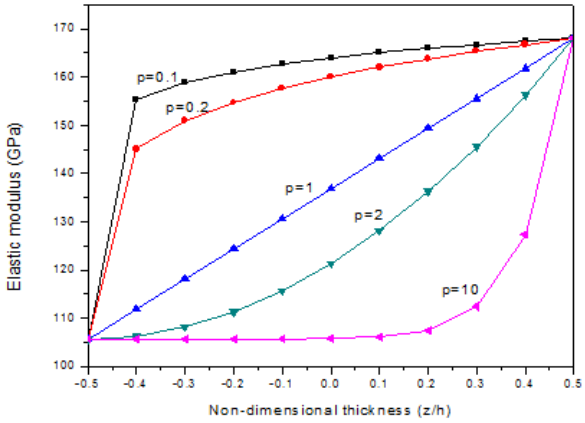

Fig. 2 Variation of elastic modulus versus non-dimensional thickness of FG plate in room temperature field and different values of grading index (p)

$$\alpha = m\pi / a \quad , \quad \beta = n\pi / b \tag{33}$$

where $i = \sqrt{-1}$, ω is the natural frequency, and (U_{mn}, V_{mn}, W_{mn}, X_{mn}, Z_{mn}) are the unknown maximum displacement coefficients.

Substituting equations (32) into equation (18), the analytical solutions can be determined by

$$\left(\begin{bmatrix} a_{11} & a_{12} & a_{13} & a_{14} & a_{15} \\ a_{12} & a_{22} & a_{23} & a_{24} & a_{25} \\ a_{13} & a_{23} & a_{33} & a_{34} & a_{35} \\ a_{14} & a_{24} & a_{34} & a_{44} & a_{45} \\ a_{15} & a_{25} & a_{35} & a_{45} & a_{55} \end{bmatrix} - \omega^2 \begin{bmatrix} M_{11} & 0 & M_{13} & M_{14} & 0 \\ 0 & M_{22} & M_{23} & M_{24} & 0 \\ M_{13} & M_{23} & M_{33} & M_{34} & M_{35} \\ M_{14} & M_{24} & M_{34} & M_{44} & 0 \\ 0 & 0 & M_{35} & 0 & M_{55} \end{bmatrix} \right) \begin{Bmatrix} U_{mn} \\ V_{mn} \\ W_{mn} \\ X_{mn} \\ Z_{mn} \end{Bmatrix} = \begin{Bmatrix} 0 \\ 0 \\ 0 \\ 0 \\ 0 \end{Bmatrix} \tag{34}$$

where a_{ij} and M_{ij} are given in Appendix.

4. Results and discussion

In this paper, numerical results are presented to illustrate the effect of temperature on the free vibration of FG plates using a new hyperbolic shear deformation plate theory including the stretching effect. With self-developed Maple's code, various examples are presented to verify the accuracy and efficiency of the present theory in predicting the free vibration responses of simply supported FG plates in thermal environments.

4.1 Thermal environment, temperature distributions and material properties

According to the above literature, temperature distribution has a significant influence on the behavior of the FGM plate. Thermal and mechanical properties of the FGMs subjected to high perform surgering temperature have importantly been affected by the temperature variation. For example, Young's modulus of stainless steel, nickel, Ti-6Al-4V, and zirconia is reduced by 37%, 21%, 34% and 31%, respectively, when the temperature rises from room temperature 300–1000(K) (Yang and Shen 2003). The real structural response of functionally graded plate required to account the temperature dependency of the material properties and temperature distribution through the thickness of the plate. The variation of Young modulus in FG plates through the thickness in room temperature, uniform, linear, nonlinear and sinusoidal thermal conditions is presented in Figs. 2-5, respectively.

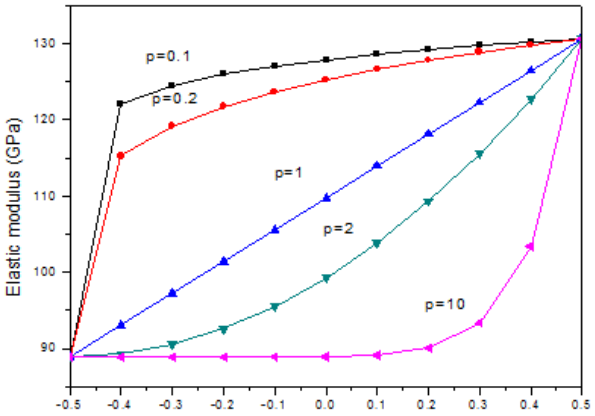

Fig. 3 Variation of elastic modulus versus non-dimensional thickness of FG plate in linear temperature field and different values of grading index (p)

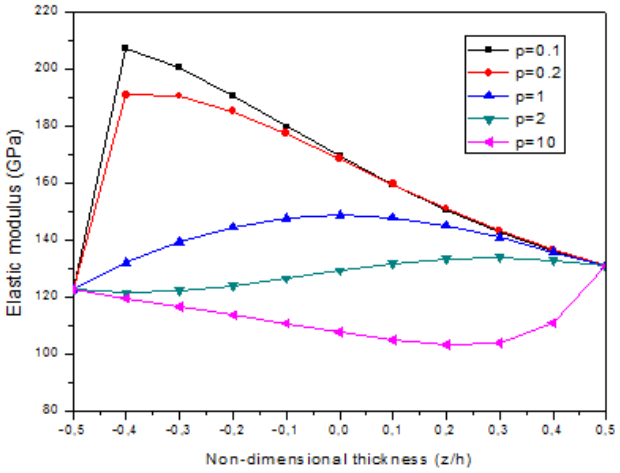

Fig. 4 Variation of elastic modulus versus non-dimensional thickness of FG plate in non linear temperature field and different values of grading index (p)

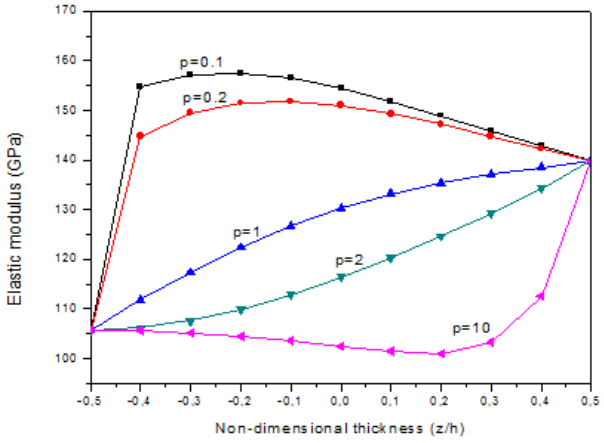

Fig. 5 Variation of elastic modulus versus non-dimensional thickness of FG plate in sinusoidal temperature field and different values of grading index (p).

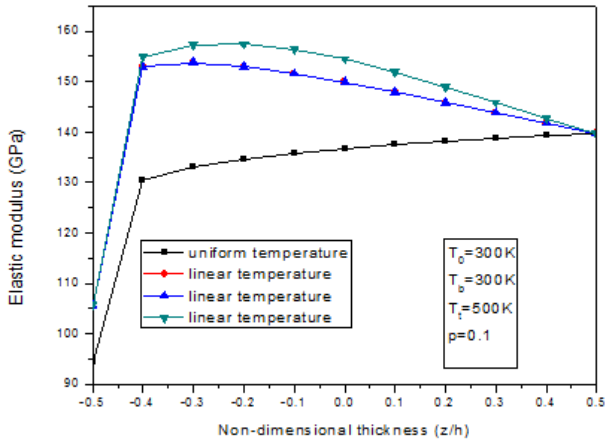

Fig. 6 Variation of elastic modulus versus non-dimensional thickness of FG plate in uniform, linear, nonlinear and sinusoidal temperature field

Room temperature is defined at T_0=300(K) for all thermal conditions. The temperature rise in linear temperature is T_b = T_t = 600(K), the nonlinear thermal conditions are T_b = 0(K) and T_t=600(K) and the sinusoidal thermal conditions are T_b=300(K) and T_t=300(K).

Figs. 2 and 3 show that the variation of elastic Young's modulus of functionally graded plates on room temperature and linear temperature variation with the volume fraction index. It is seen from the above figures that Young's modulus is similar for conditions with room temperature and uniform temperature, but the graphs move to smaller values with the uniform temperature rise. It is clear that Young's modulus decreases with increasing the power law index. In addition, it can be observed from Figs. 4 and 5 that the behavior of Young's modulus in nonlinear and sinusoidal thermal loads is completely different from that in room and linear temperature cases. The value of Young's modulus increases close to the lower surface, then decreases when p<1, and the modulus decreases when $1 \leq p <10$. However, Young's modulus decreases then increases close to upper surface for the large value of grading index p>10. Thus, it can be concluded that the environmental conditions type has a considerable effect on Young's modulus. A comparison study on Young's modulus is carried out for uniform, linear, nonlinear and sinusoidal thermal conditions in Fig. 6.

4.2 Validation of the results

4.2.1 Validation

In this section, the accuracy of the presented refined hyperbolic plate theory with stretching effect ($\varepsilon_z \neq 0$) having five unknowns only for the free vibration of the temperature-dependent FG plates only is demonstrated by comparing the present solution with those of other available results in the literature of higher-order shear deformation theories those of Taleb *et al*. (2018), Huang and Shen (2004) and Shahrjerdi *et al*. (2011) without stretching effect and with more unknowns (Huang and Shen, 2004, Shahrjerdi *et al*. 2011). In addition, the influences various parameters like power law index parameter p, shear deformation, temperature distribution on vibration response of functionally graded plate have been investigated. The nondimensional frequency parameter is taken as, where and is at (Huang and Shen, 2004, Shahrjerdi *et al*. 2011). Two types of FGMs are considered: (ZrO_2/Ti-6Al-4V) and (Si_3N_4/ SUS304). The description of material properties used in the analysis are listed in Table 1.

Example 1

The first example aims to verify the accuracy of the present theory in predicting the natural frequency parameters of FG plates in thermal environment. A comparison of the first non-dimensional natural frequency parameters is realized for a (ZrO_2/Ti-6Al-4V) FG plate in thermal environments are tabulated in Table 2. The FG plate is made of titanium alloy (Ti-6Al-4V) on its lower surface and zirconium oxide (ZrO) on its upper surface. For this end, the geometric of FG plates is taken as: h = 0.0025 m, a=b=0.2 m. An identical value of Poisson's ratio v=0.3 is assumed for both ceramic and metal. The validation of the proposed refined hyperbolic plate model with stretching effect ($\varepsilon_z \neq 0$) is carried out by comparing the obtained results with those computed via four variable hyperbolic shear deformation plate theory obtained by Taleb *et al*. (2018), the second order shear deformation plate theory (SSDT) developed by Shahrjerdi *et al*. (2011) and the higher-order shear deformation plate theory (HSDT) developed by Huang and Shen (2004).

As clearly shown in Table 2, the results of the four variable hyperbolic shear deformation plate theory obtained by Taleb *et al*. (2018), the (SSDT) plate theory developed by Shahrjerdi *et al*. (2011) and the (HSDT) plate theory developed by Huang and Shen (2004) are in a good agreement with the present results of refined hyperbolic plate theory with stretching effect ($\varepsilon_z \neq 0$) and these for all values of power law index p, either for the case of temperature-dependent and temperature-independent FG plates. Also, inspection of Tables 2 reveals that the dimensionless fundamental frequencies of the FG plate decreases with the increase of power law index p and the temperature rise decreases the dimensionless fundamental frequencies. The inclusion of thickness stretching effect ($\varepsilon_z \neq 0$) makes a FG plates stiffer, and hence, leads to increase slightly of the natural frequency.

Example 2

In the second example, a FG (Si_3N_4/ SUS304) plate is examined. For this materials, the Poisson's ratio is taken v=0.28. The dimensionless fundamental frequencies obtained by the proposed refined hyperbolic plate model with stretching effect ($\varepsilon_z \neq 0$) are compared with the published results of the four variable refined hyperbolic plate theory obtained by Taleb *et al*. (2018), Shahrjerdi *et al*. (2011) and Huang and Shen (2004) in Table 3 for different values of power law index p. It can be seen that the fundamental frequency values computed from present model are in a good agreement with those reported by Taleb *et al*. (2018), Shahrjerdi *et al*. (2011) and Huang and Shen (2004). Also , the inclusion of thickness stretching effect ($\varepsilon_z \neq 0$) makes a FG plates stiffer, and hence, leads to increase of the natural frequency.

Table 2 Non-dimensional natural frequency parameter of simply supported (ZrO_2/Ti-6Al-4V) FG plate in thermal environments

Mode (1,1) Natural frequency of $(ZrO_2/Ti-6Al-4V)$ FG plate		$T_b = 300(K)$				
			$T_t = 400(K)$		$T_t = 600(K)$	
		$T_t = 300(K)$	Temperature-dependent	Temperature-independent	Temperature-dependent	Temperature-independent
ZrO_2	SSDT[(a)] $\varepsilon_z = 0$	8.333	7.614	7.892	5.469	6.924
	TSDT [(b)] $\varepsilon_z = 0$	8.273	7.886	8.122	6.685	7.686
	RSDT[(c)] $\varepsilon_z = 0$	8.288	7.818	8.070	6.547	7.613
	Present $\varepsilon_z \neq 0$	8.478	7.919	8.189	6.305	7.578
$p = 0.5$	SSDT[(a)] $\varepsilon_z = 0$	7.156	6.651	6.844	5.255	6.175
	TSDT [(b)] $\varepsilon_z = 0$	7.139	6.876	7.154	6.123	6.776
	RSDT[(c)] $\varepsilon_z = 0$	7.120	6.791	6.968	5.941	6.656
	Present $\varepsilon_z \neq 0$	7.288	6.896	7.088	5.832	6.672
$p = 1$	SSDT[(a)] $\varepsilon_z = 0$	6.700	6.281	6.446	5.167	5.904
	TSDT [(b)] $\varepsilon_z = 0$	6.657	6.435	6.592	5.819	6.362
	RSDT[(c)] $\varepsilon_z = 0$	6.665	6.383	6.537	5.675	6.275
	Present $\varepsilon_z \neq 0$	6.825	6.491	6.658	5.608	6.309
$p = 2$	SSDT[(a)] $\varepsilon_z = 0$	6.333	5.992	6.131	5.139	5.711
	TSDT [(b)] $\varepsilon_z = 0$	6.286	6.101	6.238	5.612	6.056
	RSDT[(c)] $\varepsilon_z = 0$	6.294	6.055	6.189	5.476	5.974
	Present $\varepsilon_z \neq 0$	6.445	6.163	6.308	5.449	6.023
Ti-6Al-4V	SSDT[(a)] $\varepsilon_z = 0$	5.439	5.103	5.333	4.836	5.115
	TSDT [(b)] $\varepsilon_z = 0$	5.400	5.322	5.389	5.118	5.284
	RSDT[(c)] $\varepsilon_z = 0$	5.410	5.290	5.357	5.097	5.250
	Present $\varepsilon_z \neq 0$	5.533	5.398	5.463	5.188	5.321

(a) Shahrjerdi *et al*. (2011)
(b) Huang and Shen (2004)
(c) Taleb *et al.* (2018)

Example 3

In the section, the comparison is performed for (ZrO_2/Ti-6Al-4V) FG plate. This example aims to verify the obtained results with those obtained by Taleb *et al*. (2018) using the four variable hyperbolic refined plate theory, the (SSDT) of Shahrjerdi *et al*. (2011) and (HSDT) of Huang and Shen (2004). The non-dimensional fundamental frequency is given in Table 4 for different vibration mode. For the modes (*m*, *n*), the integers *m* and *n* denote the number of half-waves in the *x* and *y* directions, respectively. It is observed that the present refined hyperbolic plate theory with stretching effect ($\varepsilon_z \neq 0$) is in a good agreement with the previously published results (Taleb *et al.* 2018, Shahrjerdi *et al*. 2011, Huang and Shen 2004) and these for different considered shape mode.

Example 4

In order to verify the accuracy of the present theory for large value of volume fraction index *p* and different values of thermal loads, an (Si_3N_4/ SUS304) FG plate is now examined. The nondimensional frequencies for FG (Si_3N_4/ SUS304) plates predicted by Shahrjerdi *et al*. (2011) using second order shear deformation theory (SSDT), and present theory are presented in Table 5. An excellent agreement between the results predicted by (SSDT) of Shahrjerdi *et al*. (2011), Taleb *et al.* (2018) and present theory is observed. It should be noted that the present theory contains five unknowns with stretching effect ($\varepsilon_z \neq 0$) as against seven in the case of (SSDT) of Shahrjerdi *et al*. (2011). It can be concluded that the present theory is not only accurate but also efficient and simple in predicting the free vibration responses of FG plates in thermal environment.

Table 3 Non-dimensional natural frequency parameter of simply supported (Si_3N_4/ SUS304) FG plate in thermal environments

Mode (1,1) Natural frequency of $(Si_3N_4/SUS304)$ FG plate		$T_b = 300(K)$ $T_t = 300(K)$	$T_b = 300(K)$ $T_t = 400(K)$ Temperature-dependent	$T_b = 300(K)$ $T_t = 400(K)$ Temperature-independent	$T_b = 300(K)$ $T_t = 600(K)$ Temperature-dependent	$T_b = 300(K)$ $T_t = 600(K)$ Temperature-independent
Si_3N_4	SSDT[a] $\varepsilon_z = 0$	12.506	12.175	12.248	11.461	11.716
	TSDT [b] $\varepsilon_z = 0$	12.495	13.397	12.382	11.984	12.213
	RSDT[c] $\varepsilon_z = 0$	12.519	12.319	12.389	11.899	12.126
	Present $\varepsilon_z \neq 0$	12.749	12.513	12.586	12.012	12.254
$p = 0.5$	SSDT[a] $\varepsilon_z = 0$	8.652	8.361	8.405	7.708	7.887
	TSDT [b] $\varepsilon_z = 0$	8.675	8.615	8.641	8.269	8.425
	RSDT[c] $\varepsilon_z = 0$	8.617	8.461	8.507	8.127	8.281
	Present $\varepsilon_z \neq 0$	8.782	8.596	8.643	8.190	8.358
$p = 1$	SSDT[a] $\varepsilon_z = 0$	7.584	7.306	7.342	6.674	6.834
	TSDT [b] $\varepsilon_z = 0$	7.555	7.474	7.514	7.171	7.305
	RSDT[c] $\varepsilon_z = 0$	7.551	7.406	7.444	7.090	7.225
	Present $\varepsilon_z \neq 0$	7.698	7.523	7.563	7.137	7.286
$p = 2$	SSDT[a] $\varepsilon_z = 0$	6.811	6.545	6.575	5.929	6.077
	TSDT [b] $\varepsilon_z = 0$	6.777	6.693	6.728	6.398	6.523
	RSDT[c] $\varepsilon_z = 0$	6.777	6.638	6.670	6.330	6.454
	Present $\varepsilon_z \neq 0$	6.906	6.738	6.773	6.362	6.499
SUS304	SSDT[a] $\varepsilon_z = 0$	5.410	5.161	5.178	4.526	4.682
	TSDT [b] $\varepsilon_z = 0$	5.405	5.311	5.335	4.971	5.104
	RSDT[c] $\varepsilon_z = 0$	5.415	5.278	5.300	4.929	5.061
	Present $\varepsilon_z \neq 0$	5.515	5.346	5.369	4.922	5.066

(a) Shahrjerdi *et al*. (2011)
(b) Huang and Shen (2004)
(c) Taleb *et al.* (2018)

4.2.2 Numerical results of present study

In the view of previous sections, it is can be seen that the proposed theory delivers results which are in good agreement with the four variable hyperbolic refined plate theory obtained by Taleb *et al.* (2018), the second order shear deformation plate theory (SSDT) developed by Shahrjerdi *et al*. (2011) and the higher-order shear deformation plate theory (HSDT) developed by Huang and Shen (2004) of the vibrated FG plate in thermal environment. In this example, the effects different parameters such as the power law index *p*, the mode numbers, and temperature fields on the free vibration responses of FG plates are investigated here. All predicted results are carried out using present refined hyperbolic plate theory with stretching effect ($\varepsilon_z \neq 0$) and compared with the four variable hyperbolic refined plate theory obtained by Taleb *et al.* (2018) without stretching effect ($\varepsilon_z \neq 0$) with the same shape function for each theory.

Table 6 show the non-dimensional frequencies values in (ZrO_2/Ti-6Al-4V) FG plate for different thermal loads. The non-dimensional natural frequency parameter is defined as $\bar{\omega} = \omega\left(a^2/h\right)\sqrt{\rho_b\left(1-\nu^2\right)/E_b}$, where E_b and ρ_b are at T_0=300(K) (Shahrjerdi *et al*. 2011). To see the effect of the power index p on the frequencies, the same values of the thermal load and the shape mode are considered. It is observed that the result for plates is in between those for pure material plates, because Young's modulus increases from pure metal to pure ceramic. Also, the frequencies decrease by increasing the temperature difference between top and bottom surfaces for the same value of power law index and shape mode that represent the effects of thermal loads. The difference

Table 4 Non-dimensional frequency parameter of simply supported (ZrO_2 / Ti-6Al-4V) FG plate in thermal environments (p=2)

Mode numbers of $(ZrO_2/Ti\text{-}6Al\text{-}4V)$ FG plate		$T_b = 300(K)$				
			$T_t = 400(K)$		$T_t = 600(K)$	
		$T_t = 300(K)$	Temperature-dependent	Temperature-independent	Temperature-Dependent	Temperature-Independent
(1,1)	SSDT[(a)] $\varepsilon_z = 0$	6.333	5.992	6.132	5.139	5.711
	TSDT [(b)] $\varepsilon_z = 0$	6.286	6.101	6.238	5.612	6.056
	RSDT[(c)] $\varepsilon_z = 0$	6.294	6.055	6.189	5.476	5.974
	Present $\varepsilon_z \neq 0$	8.478	6.163	6.308	5.449	6.023
(1,2)	SSDT[(a)] $\varepsilon_z = 0$	14.896	14.383	14.684	13.260	14.253
	TSDT [(b)] $\varepsilon_z = 0$	14.625	14.372	14.655	13.611	14.474
	RSDT[(c)] $\varepsilon_z = 0$	14.699	14.301	14.588	13.453	14.363
	Present $\varepsilon_z \neq 0$	15.073	14.622	14.927	13.633	14.633
(2,2)	SSDT[(a)] $\varepsilon_z = 0$	22.608	21.942	22.386	20.557	21.935
	TSDT [(b)] $\varepsilon_z = 0$	21.978	21.653	22.078	20.652	21.896
	RSDT[(c)] $\varepsilon_z = 0$	22.197	21.663	22.082	20.581	21.849
	Present $\varepsilon_z \neq 0$	22.784	22.190	22.633	20.958	22.330
(1,3)	SSDT[(a)] $\varepsilon_z = 0$	27.392	26.630	27.163	25.077	26.700
	TSDT [(b)] $\varepsilon_z = 0$	26.454	26.113	26.605	24.961	26.435
	RSDT[(c)] $\varepsilon_z = 0$	26.811	26.190	26.689	24.954	26.446
	Present $\varepsilon_z \neq 0$	27.534	26.850	27.377	25.453	27.059
(2,3)	SSDT[(a)] $\varepsilon_z = 0$	34.106	33.211	33.867	31.425	33.384
	TSDT [(b)] $\varepsilon_z = 0$	32.659	32.239	32.840	30.904	32.664
	RSDT[(c)] $\varepsilon_z = 0$	33.271	32.540	33.148	31.118	32.904
	Present $\varepsilon_z \neq 0$	34.192	33.393	34.034	31.803	33.715

(a) Shahrjerdi *et al*. (2011)
(b) Huang and Shen (2004)
(c) Taleb *et al.* (2018)

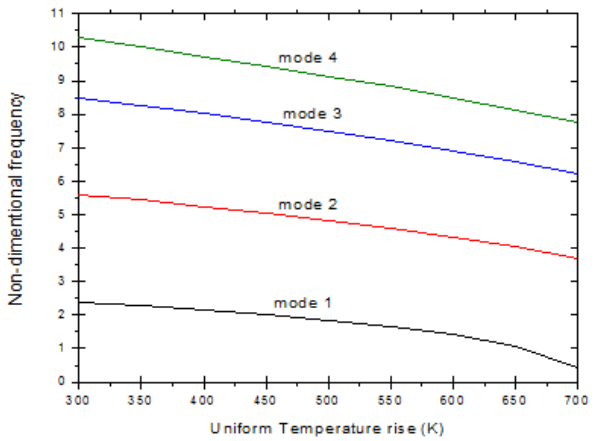

Fig. 7 First four Non-dimensional frequency parameters versus uniform temperature field for simply supported (ZrO2/Ti-6Al-4V) FGP when a / h = 10 and a = 0.2, p = 1

between temperature-dependent and independent FG plates is less significant, tables 6 reveals the smaller frequencies in temperature-dependent FG plates, which proves the accuracy and effectiveness of temperature-dependent material properties.

The variation of the first four frequencies as a function of uniform, linear, nonlinear and sinusoidal temperature fields in simply supported FG plate is plotted in Figs. 7-10. The combination of (ZrO_2/Ti-6Al-4V) (Table 1) is assumed with material and geometric parameters of p=1, a=b=0.2 and a/h=10. The non-dimensional natural frequency parameter is defined as $\bar{\omega} = \omega\left(b^2/\pi^2\right)\sqrt{I_0/D_0}$, where I_0= ρh and $D_0 = Eh^3/12\left(1-\nu^2\right)$ and it is noted that ρ, v and E are chosen to be the values of (ZrO_2/Ti-6Al-4V) evaluated at the room temperature. As expected, the frequencies are reduced with increasing temperature and this is due to the decrease of Young's modulus with rising temperatures.

Table 5 Non-dimensional natural frequency of temperature dependent (Si_3N_4/SUS304) FG plate for different volume fraction index p in thermal environments, Mode (1, 1)

Thermal Loads $T_0 = 300$ (K), $b = a = 0.2$, $h = 0.025$		$T_b = 300(K)$ $T_t = 300(K)$	$T_b = 300(K)$ $T_t = 400(K)$	$T_b = 300(K)$ $T_t = 600(K)$
Si_3N_4	SSDT(a) $\varepsilon_z = 0$	12.506	12.175	11.461
	RSDT(b) $\varepsilon_z = 0$	12.519	12.319	11.899
	Present $\varepsilon_z \neq 0$	12.749	12.513	12.012
$p = 0.5$	SSDT(a) $\varepsilon_z = 0$	8.652	8.361	7.708
	RSDT(b) $\varepsilon_z = 0$	8.617	8.461	8.127
	Present $\varepsilon_z \neq 0$	8.782	8.596	8.190
$p = 10$	SSDT(a) $\varepsilon_z = 0$	5.907	5.645	5.031
	RSDT(b) $\varepsilon_z = 0$	5.868	5.731	5.412
	Present $\varepsilon_z \neq 0$	5.975	5.809	5.419
$p = 20$	SSDT(a) $\varepsilon_z = 0$	5.711	5.450	4.825
	RSDT(b) $\varepsilon_z = 0$	5.676	5.540	5.210
	Present $\varepsilon_z \neq 0$	5.781	5.613	5.212
$p = 40$	SSDT(a) $\varepsilon_z = 0$	5.591	5.329	4.694
	RSDT(b) $\varepsilon_z = 0$	5.558	5.420	5.083
	Present $\varepsilon_z \neq 0$	5.660	5.492	5.082
SUS304	SSDT(a) $\varepsilon_z = 0$	5.410	5.161	4.526
	RSDT(b) $\varepsilon_z = 0$	5.415	5.278	4.929
	Present $\varepsilon_z \neq 0$	5.515	5.346	4.922

(a) Shahrjerdi *et al*. (2011)
(b) Taleb *et al.* (2018)

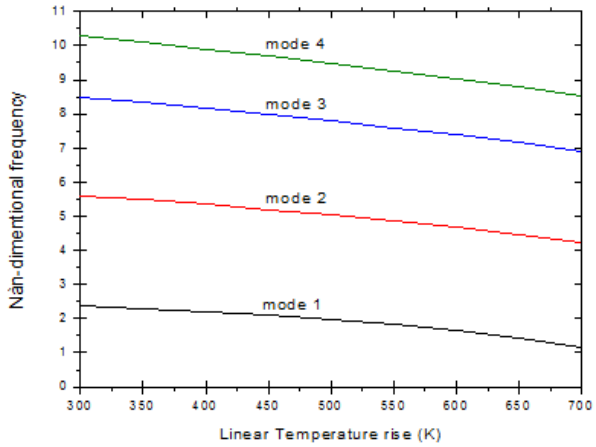

Fig. 8 First four Non-dimensional frequency parameters versus linear temperature field for simply supported (ZrO2/Ti-6Al-4V) FGP when a / h = 10 and a = 0.2, p = 1

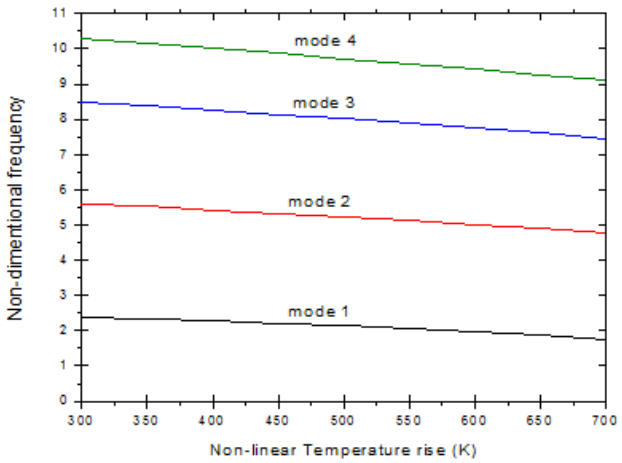

Fig. 9 First four Non-dimensional frequency parameters versus non-linear temperature field for simply supported (ZrO2/Ti-6Al-4V) FGP when a / h = 10 and a = 0.2, p = 1

It can be seen that the decreasing slope of frequencies in lower modes is smaller than those in higher modes. At the same temperature, we note that the difference between two consecutive lower modes is greater than that in two consecutive higher modes.

5. Conclusion

The new hyperbolic shear deformation plate theory including the stretching effect proposed by the authors, is

Table 6 Non-dimensional natural frequency parameter of simply supported (ZrO_2/Ti-6Al-4V) FG plate in thermal environments and for different modes of vibration

Mode numbers of FGP (ZrO_2 and Ti-6Al-4V)		$T_t = 300(K)$	$T_b = 300(K)$ $T_t = 400(K)$		$T_t = 600(K)$	
			Temperature-dependent	Temperature-independent	Temperature-dependent	Temperature-independent
ZrO_2	(1,1)	8.478 8.478	6.163 6.163 6.163	6.308	5.449	6.023
	(1,2)	19.862	18.999	19.558	16.945	18.935
	(2,2)	30.065	28.930	29.749	26.432	29.106
	(1,3)	36.361	35.050	36.031	32.244	35.363
	(2,3)	45.195	43.653	44.860	40.473	44.182
$p = 0.5$	(1,1)	7.288	6.896	7.088	5.832	6.672
	(1,2)	17.091	16.481	16.881	15.080	16.454
	(2,2)	25.890	25.090	25.673	23.373	25.234
	(1,3)	31.325	30.403	31.099	28.470	30.641
	(2,3)	38.957	37.878	38.728	35.686	38.266
$p = 1$	(1,1)	6.825	6.491	6.658	5.608	6.309
	(1,2)	15.994	15.469	15.818	14.284	15.459
	(2,2)	24.215	23.526	24.032	22.065	23.663
	(1,3)	29.289	28.495	29.098	26.847	28.713
	(2,3)	36.410	35.483	36.218	33.612	35.830
$p = 2$	(1,1)	6.445	6.163	6.308	5.449	6.023
	(1,2)	15.073	14.622	14.927	13.633	14.633
	(2,2)	22.784	22.190	22.633	20.958	22.330
	(1,3)	27.534	26.850	27.377	25.453	27.059
	(2,3)	34.192	33.393	34.034	31.803	33.715
Ti-6Al-4V	(1,1)	5.533	5.398	5.463	5.188	5.321
	(1,2)	12.963	12.724	12.890	12.303	12.741
	(2,2)	19.623	19.292	19.546	18.682	19.392
	(1,3)	23.732	23.343	23.652	22.616	23.491
	(2,3)	29.498	29.030	29.417	28.140	29.253

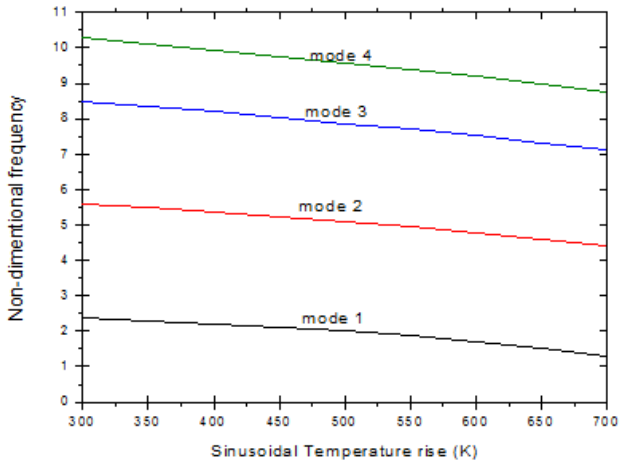

Fig. 10 First four Non-dimensional frequency parameters versus sinusoidal temperature field for simply supported (ZrO2/Ti-6Al-4V) FGP when $a / h = 10$ and a = 0.2, p = 1

implemented in this study to analyze the free vibration for simply supported FGM in thermal environments and developed for temperature-dependent FG plates subjected to uniform, linear, nonlinear, and sinusoidal temperature fields. The proposed theory satisfies free transverse shear stress at the top and bottom surfaces of the plate, and takes into account stretching effect in thickness direction, thus the numerical results show a good agreement with which is available from related literature. Material properties of FG plates are assumed to be temperature-dependent and graded through the thickness according to a power-law distribution in terms of volume fractions of constituents. By considering further simplifying suppositions to the existing higher order shear deformation theory, with incorporation of an undetermined integral term, the present theory has only five unknowns, which is even less than the other shear deformation theories including stretching effect, and hence, make this model simple and efficient to employ. The equation of motion of the vibrated structure obtained via the

classical Hamilton's principle and solved using Navier's steps. The subsequent main points can be drawn from the present study:

(1) The accuracy of the present work is ascertained by comparing it with existing shear deformation theory and excellent agreement was observed.

(2) The frequency decreases as temperature change increases in all types of temperature fields.

(3) The present novel hyperbolic shear deformation plate theory is not only accurate but also simple in predicting the vibration analysis of FG plates in thermal environment.

(4) The inclusion of thickness stretching effect ($\varepsilon_z \neq 0$) makes a FG plates stiffer, and hence, leads to increase of the natural frequency.

(5) The thickness stretching effect plays a significant role in moderately thick and thick FG plates and it needs to be taken in consideration in the modeling.

Finally, the formulation lends itself particularly well to study several problems related to the bending, vibration and dynamic behavior of isotropic, classical and advanced composite macro/nanostructures (Youzera *et al*. 2017, Draiche *et al*. 2019, Karami *et al*. 2019abcd, Khiloun *et al*. 2019).

References

Adhikari, B., and Singh, B. N. (2019), "Dynamic response of functionally graded plates resting on two-parameter-based elastic foundation model using a quasi-3D theory", *Mech. Based Design Struct. Machines*, 1-31. https://doi.org/10.1080/15397734.2018.1555965.

Akbaş, Ş.D. (2017), "Vibration and static analysis of functionally graded porous plates", *J. Appl. Comput. Mech.*, **3**(3), 199-207. https://doi.org/10.22055/JACM.2017.21540.1107.

Alibeigloo, A., and Alizadeh, M. (2015), "Static and free vibration analyses of functionally graded sandwich plates using state space differential quadrature method", *J. Mech. Solids*, **54**, 252-266. https://doi.org/10.1016/j.euromechsol.2015.06.011.

Attia, A., Tounsi, A., Bedia, E.A. and Mahmoud, S.R. (2015), "Free vibration analysis of functionally graded plates with temperature-dependent properties using various four variable refined plate theories", *Steel Compos. Struct*., **18**(1), 187-212. https://doi.org/10.12989/scs.2015.18.1.187.

Berghouti, H., Adda Bedia, E.A. Benkhedda, A. and Tounsi, A. (2019), "Vibration analysis of nonlocal porous nanobeams made of functionally graded material", *Adv. Nano Res.,* **7**(5), 351-364. https://doi.org/10.12989/anr.2019.7.5.351.

Bourada, F., Bousahla, A.A., Bourada, M., Azzaz, A., Zinata, A., Tounsi, A. (2019), "Dynamic investigation of porous functionally graded beam using a sinusoidal shear deformation theory", *Wind Struct.*, **28**(1), 19-30. https://doi.org/10.12989/was.2019.28.1.019

Carrera, E., Brischetto, S., Cinefra, M., and Soave, M. (2011), "Effects of thickness stretching in functionally graded plates and shells", *Compos. Part B Eng.*, **42**(2), 123-133. https://doi.org/10.1016/j.compositesb.2010.10.005.

Chakraverty, S., and Pradhan, K. K. (2014), "Free vibration of exponential functionally graded rectangular plates in thermal environment with general boundary conditions", *Aerosp. Sci. Technol.*, **36**, 132-156. https://doi.org/10.1016/j.ast.2014.04.005.

Cui, D. and Hu, H. (2016), "Thermal buckling and natural vibration of a rectangular thin plate with in-plane stick-slip-stop boundaries", *J. Vib. Control*., **22**(7), 1950-1966. https://doi.org/10.1177/1077546314546394.

Daikh, A. A. (2019), "Temperature dependent vibration analysis of functionally graded sandwich plates resting on Winkler/Pasternak/Kerr foundation", *Mater. Res. Express*, **6**(6), 065702. https://doi.org/10.1088/2053-1591/ab097b.

Darilmaz, K. (2015), "Vibration analysis of functionally graded material (FGM) grid systems", *Steel Compos. Struct., Int. J.*, **18**(2), 395-408. https://doi.org/10.12989/scs.2015.18.2.395.

Darilmaz, K., Aksoylu, M.G. and Durgun, Y. (2015), "Buckling analysis of functionally graded material grid systems", *Struct. Eng. Mech., Int. J.*, **54**(5), 877-890. https://doi.org/10.12989/sem.2015.54.5.87.

Draiche, K., Bousahla, A. A., Tounsi, A., Alwabli, A. S., Tounsi, A., and Mahmoud, S. R. (2019), "Static analysis of laminated reinforced composite plates using a simple first-order shear deformation theory", *Comput. Concrete*, **24**(4), 369-378. https://doi.org/10.12989/cac.2019.24.4.36.

Ebrahimi, F. (2013), "Analytical investigation on vibrations and dynamic response of functionally graded plate integrated with piezoelectric layers in thermal environment", *Mech. Adv. Mater. Struct*., **20**(10), 854-870. https://doi.org/10.1080/15376494.2012.677098.

Ebrahimi, F., Jafari, A. (2016), "Thermo-mechanical vibration analysis of temperature-dependent porous FG beams based on Timoshenko beam theory", *Struct. Eng. Mech.*, **59**(2), 343-371. https://doi.org/10.12989/sem.2016.59.2.34.

El Meiche, N., Tounsi, A., Ziane, N., and Mechab, I. (2011), "A new hyperbolic shear deformation theory for buckling and vibration of functionally graded sandwich plate", *J. Mech. Sci.*, **53**(4), 237-247. https://doi.org/10.1016/j.ijmecsci.2011.01.004.

Fazzolari, F. A. (2016), "Modal characteristics of P-and S-FGM plates with temperature-dependent materials in thermal environment", *J. Thermal Stress.*, **39**(7), 854-873. https://doi.org/10.1080/01495739.2016.1189772.

Huang, X. L., Shen, H. S. (2004), "Nonlinear vibration and dynamic response of functionally graded plates in thermal environments". International Journal of Solids and Structures., **41**(9), 2403-2427. https://doi.org/10.1016/j.ijsolstr.2003.11.012.

Joshi, P. V., Jain, N. K., Ramtekkar, G. D., and Virdi, G. S. (2016), "Vibration and buckling analysis of partially cracked thin orthotropic rectangular plates in thermal environment", *Thin Wall. Struct.*, **109**, 143-158. https://doi.org/10.1016/j.tws.2016.09.020.

Kant, T. (1993), "A critical review and some results of recently developed refined theories of fiber-reinforced laminated composites and sandwiches", *Compos. Struct*., **23**(4), 293-312. https://doi.org/10.1016/0263-8223(93)90230-N.

Kant, T., and Swaminathan, K. (2001), "Free vibration of isotropic, orthotropic, and multilayer plates based on higher order refined theories", Journal of Sound and Vibration., **241**(2), 319-327. https://doi.org/10.1006/jsvi.2000.3232.

Kar, V.R., Panda, S.K. (2014), "Large deformation bending analysis of functionally graded spherical shell using FEM", *Struct. Eng. Mech., Int. J.*, **53**(4), 661 - 679. https://doi.org/10.12989/sem.2015.53.4.661.

Kar, V.R. and Panda, S.K. (2015), "Nonlinear flexural vibration of shear deformable functionally graded spherical shell panel", Steel Compos. Struct., Int. J., **18**(3), 693-709. https://doi.org/10.12989/scs.2015.18.3.693.

Karami, B., Janghorban, M., Shahsavari, D., and Tounsi, A. (2018), "A size-dependent quasi-3D model for wave dispersion analysis of FG nanoplates", *Steel and Compos. Struct*, **28**(1), 99-110. https://doi.org/10.12989/scs.2018.28.1.099.

Karami, B., Janghorban, M., Tounsi, A. (2018b), "Nonlocal strain

gradient 3D elasticity theory for anisotropic spherical nanoparticles", *Steel Compos. Struct*, **27**(2), 201-216. https://doi.org/10.12989/scs.2018.27.2.20.

Karami, B., Janghorban, M. and Tounsi, A. (2019a), "Galerkin's approach for buckling analysis of functionally graded anisotropic nanoplates/different boundary conditions", *Eng. Comput.*, **35**, 1297-1316. https://doi.org/10.1007/s00366-018-0664-9.

Karami, B., Shahsavari, D., Janghorban, M., and Tounsi, A. (2019b), "Resonance behavior of functionally graded polymer composite nanoplates reinforced with graphene nanoplatelets", *J. Mech. Sci.*, **156**, 94-105. https://doi.org/10.1016/j.ijmecsci.2019.03.036.

Karami, B., Janghorban, M., and Tounsi, A. (2019c), "Wave propagation of functionally graded anisotropic nanoplates resting on Winkler-Pasternak foundation", *Struct. Eng. Mech.*, **70**(1), 55-66. https://doi.org/10.12989/sem.2019.70.1.055.

Karami, B., Janghorban, M. and Tounsi, A. (2019d), "On exact wave propagation analysis of triclinic material using three-dimensional bi-Helmholtz gradient plate model", *Struct. Eng. Mech.*, **69**(5), 487-497. https://doi.org/10.12989/sem.2019.69.5.487.

Khalili, S. M. R., and Mohammadi, Y. (2012), "Free vibration analysis of sandwich plates with functionally graded face sheets and temperature-dependent material properties: A new approach", *European J. Mech.-A/Solids*, **35**, 61-74. https://doi.org/10.1016/j.euromechsol.2012.01.003.

Khiloun, M., Bousahla, A. A., Kaci, A., Bessaim, A., Tounsi, A., and Mahmoud, S. R. (2019), "Analytical modeling of bending and vibration of thick advanced composite plates using a four-variable quasi 3D HSDT", *Eng. Comput*, 1-15. https://doi.org/10.1007/s00366-019-00732-1.

Kim, Y. W. (2005), "Temperature dependent vibration analysis of functionally graded rectangular plates", *J. Sound Vib.*, **284**(3-5), 531-549. https://doi.org/10.1016/j.jsv.2004.06.043.

Kolahchi, R., Bidgoli, A.M.M. and Heydari, M.M. (2015), "Size-dependent bending analysis of FGM nano-sinusoidal plates resting on orthotropic elastic medium", *Struct. Eng. Mech., Int. J.*, **55**(5), 1001-1014. https://doi.org/10.12989/sem.2015.55.5.1001.

Lashkari, M. J. and Rahmani, O. (2016), "Bending analysis of sandwich plates with composite face sheets and compliance functionally graded syntactic foam core", *Proceedings of the Institution of Mechanical Engineers, Part C J. Mechanical Engineering Science*, **230**(20), 3606-3630. https://doi.org/10.1177/0954406215616417.

Li, Q., Iu, V. P. and Kou, K. P. (2008), "Three-dimensional vibration analysis of functionally graded material sandwich plates", *J. Sound Vib.*, **311**(1), 498-515. https://doi.org/10.1016/j.jsv.2007.09.018.

Mahmoudi, A., Benyoucef, S., Tounsi, A., Benachour, A., Adda Bedia, E.A., Mahmoud, S.R. (2019), "A refined quasi-3D shear deformation theory for thermo-mechanical behavior of functionally graded sandwich plates on elastic foundations", *J. Sandwich Struct. Mater.*, **21**(6), 1906-1926. https://doi.org/10.1177/1099636217727577.

Medani, M., Benahmed, A., Zidour, M., Heireche, H., Tounsi, A., Bousahla, A.A., Tounsi, A., Mahmoud, S.R. (2019), "Static and dynamic behavior of (FG-CNT) reinforced porous sandwich plate", *Steel and Compos. Struct.*, **32**(5), 595-610. https://doi.org/10.12989/scs.2019.32.5.595.

Mehar, K., and Kumar Panda, S. (2018), "Thermal free vibration behavior of FG-CNT reinforced sandwich curved panel using finite element method", *Polymer Compos.*, **39**(8), 2751-2764. https://doi.org/10.1002/pc.24266.

Neves, A. M. A., Ferreira, A. J. M., Carrera, E., Cinefra, M., Roque, C. M. C., Jorge, R. M. N. and Soares, C. M. (2013), "Static, free vibration and buckling analysis of isotropic and sandwich functionally graded plates using a quasi-3D higher-order shear deformation theory and a meshless technique", *Compos. Part B Eng.*, **44**(1), 657-674. https://doi.org/10.1016/j.compositesb.2012.01.089.

Nguyen, T.K. (2015), "A higher-order hyperbolic shear deformation plate model for analysis of functionally graded materials", *Int.J.Mech.Mater.Des.*, **11**(2), 203-219. https://doi.org/10.1007/s10999-014-9260-3.

Pandey, S., and Pradyumna, S. (2015), "Free vibration of functionally graded sandwich plates in thermal environment using a layerwise theory", *Europ. J. Mech. A Solids*, **51**, 55-66. https://doi.org/10.1016/j.euromechsol.2014.12.001.

Parida, S., and Mohanty, S. C. (2018), "Free Vibration Analysis of Functionally Graded Skew Plate in Thermal Environment Using Higher Order Theory", International Journal of Applied Mechanics, **10**(01), 1850007. https://doi.org/10.1142/S1758825118500072.

Shahrjerdi, A., Mustapha, F., Bayat, M. and Majid, D.L.A. (2011), "Free vibration analysis of solar functionally graded plates with temperature-dependent material properties using second order shear deformation theory", *J. Mech. Sci. Techol.*, **25**(9), 2195-2209. https://doi.org/10.1007/s12206-011-0610-x.

Taleb, O., Houari, M.S.A ., Bessaim, A., Tounsi, A and Mahmoud, S.R. (2018), "A new plate model for vibration response of advanced composite plates in thermal environment", *Struct. Eng. Mech.., Int. J.,* **18**(3), 693-709. https://doi.org/10.12989/sem.2018.67.4.369.

Thai, H. T., and Choi, D. H. (2013), "A simple first-order shear deformation theory for the bending and free vibration analysis of functionally graded plates", *Compos. Struct*, **101**, 332-340. https://doi.org/10.1016/j.compstruct.2013.02.019.

Tornabene, F. (2009), "Free vibration analysis of functionally graded conical, cylindrical shell and annular plate structures with a four-parameter power-law distribution", *Comput. Methods Appl. Mech. Eng.*, **198**(37-40), 2911-2935. https://doi.org/10.1016/j.cma.2009.04.011

Tu, T. M., Quoc, T. H., and Van Long, N. (2019), "Vibration analysis of functionally graded plates using the eight-unknown higher order shear deformation theory in thermal environments", *Aerosp. Sci. Technol.*, **84**, 698-711. https://doi.org/10.1016/j.ast.2018.11.010.

Van Long, N., Quoc, T. H., and Tu, T. M. (2016), "Bending and free vibration analysis of functionally graded plates using new eight-unknown shear deformation theory by finite-element method", *J. Adv. Struct. Eng.*, **8**(4), 391-399. https://doi.org/10.1007/s40091-016-0140-y.

Wang, Y. Q. and Zu, J. W. (2017), "Vibration behaviors of functionally graded rectangular plates with porosities and moving in thermal environment", *Aerosp. Sci. Technol.*, **69**, 550-562. https://doi.org/10.1016/j.ast.2017.07.023.

Wattanasakulpong, N., Prusty, G. B., and Kelly, D. W. (2013), "Free and forced vibration analysis using improved third-order shear deformation theory for functionally graded plates under high temperature loading", *J. Sandwich Struct. Mater.*, **15**(5), 583-606. https://doi.org/10.1177/1099636213495751.

Yaghoobi, H., and Yaghoobi, P. (2013), "Buckling analysis of sandwich plates with FGM face sheets resting on elastic foundation with various boundary conditions: An analytical approach", *Meccanica*, **48**(8), 2019-2035. https://doi.org/10.1007/s11012-013-9720-0.

Yang, J., Kitipornchai, S., and Liew, K. M. (2003), "Large amplitude vibration of thermo-electro-mechanically stressed FGM laminated plates", *Comput. Methods Appl. Mech. Eng.*, **192**(35-36), 3861-3885. https://doi.org/10.1016/S0045-7825(03)00387-6.

Youzera, H., Meftah, S.A., and Daya, E.M. (2017), "Superharmonic resonance of cross-ply laminates by the method

of multiple scales", *J. Comput. Nonlinear Dynam.*, **12**(5). https://doi.org/10.1115/1.4036914.

Zarga, D., Tounsi, A., Bousahla, A.A., Bourada, F., Mahmoud, S.R. (2019), "Thermomechanical bending study for functionally graded sandwich plates using a simple quasi-3D shear deformation theory", *Steel Compos. Struct.*, **32**(3), 389-410. https://doi.org/10.12989/scs.2019.32.3.389

Zaoui, F. Z., Ouinas, D. and Tounsi, A. (2019), "New 2D and quasi-3D shear deformation theories for free vibration of functionally graded plates on elastic foundations" *Compos. Part B Eng.*, **159**, 231-247. https://doi.org/10.1016/j.compositesb.2018.09.051.

Zenkour, A. M., and Sobhy, M. (2010), "Thermal buckling of various types of FGM sandwich plates", *Compos. Struct*, **93**(1), 93-102. https://doi.org/10.1016/j.compstruct.2010.06.012.

CC

Appendix

The stiffness and inertia coefficients $\underline{a_{ij}}$ and M_{ij} appeared in governing equation (20) are as follows.

$$a_{11}=-\left(\alpha^2\left(A_{11}+A_{11}^T\right)+\beta^2\left(A_{22}^T+A_{66}\right)\right),\quad a_{12}=-\alpha\beta\left(A_{12}+A_{66}\right),\quad a_{13}=\alpha^3\left(B_{11}+B_{11}^T\right)+\alpha\beta^2\left(B_{12}+2B_{66}+B_{22}^T\right),$$

$$a_{22}=-\left(\alpha^2\left(A_{66}+A_{11}^T\right)+\beta^2\left(A_{22}^T+A_{22}\right)\right)\ a_{14}=-\alpha\left(\alpha^2\left(B_{11}^s+B_{11}^{sT}\right)k_1A'+\left(k_2B'B_{12}^s+k_1A'B_{22}^{sT}+\left(k_1A'+k_2B'\right)B_{66}^s\right)\beta^2\right),$$

$$a_{15}=L\alpha,\quad a_{23}=\beta^3\left(B_{22}+B_{22}^T\right)+\alpha^2\beta\left(B_{12}+2B_{66}+B_{22}^T\right),$$

$$a_{24}=-\beta\left(\beta^2\left(B_{22}^s+B_{22}^{sT}\right)k_2B'+\left(k_1A'B_{12}^s+\left(k_1A'+k_2B'\right)B_{66}^s+k_2B'B_{11}^{sT}\right)\alpha^2\right)\ a_{25}=L\beta$$

$$a_{33}=-\left(\alpha^4\left(D_{11}+D_{11}^T\right)+2(D_{12}+2D_{66})\alpha^2\beta^2+\left(D_{11}^T+D_{22}^T\right)\alpha^2\beta^2+\left(D_{22}+D_{22}^T\right)\beta^4+A_{11}^T\alpha^2+A_{22}^T\beta^2\right)$$

$$a_{34}=k_1A'\left(D_{11}^s\alpha^4+D_{12}^s\alpha^2\beta^2\right)+2(k_1A'+k_2B')\,D_{66}^s\alpha^2\beta^2$$
$$+k_2B'\left(D_{22}^s\beta^4+D_{12}^s\alpha^2\beta^2\right)+k_1A'\alpha^4D_{11}^{sT}+k_2B'D_{22}^{sT}+$$
$$\left(k_1A'D_{22}^{sT}+k_2B'D_{11}^{sT}\right)\alpha^2\beta^2+k_1A'\alpha^2A_{11}^T+k_2B'\beta^2A_{22}^T$$

$$a_{35}=-L^s\left(\alpha^2+\beta^2\right)-\left(E_{11}^T\alpha^2+E_{22}^T\beta^2\right)$$

$$a_{44}=\left(k_1A'\right)^2\left(H_{11}^sk_1+H_{12}^sk_2\right)\alpha^4+\left(k_1A'+k_2B'\right)^2H_{66}^s\alpha^2\beta^2$$
$$+\left(H_{22}^s+H_{22}^{sT}\right)\left(k_2B'\right)^2\beta^2+$$
$$\left(H_{11}^{sT}\left(k_2B'\right)^2+H_{22}^{sT}\left(k_1A'\right)^2+2H_{11}^sk_1k_2A'B'\right)\alpha^2\beta^2$$
$$-\left(k_1A'\right)^2\left(A_{55}^s+A_{11}^T\right)\alpha^2-\left(k_2B'\right)^2\left(A_{44}^s+A_{22}^T\right)\beta^2$$

$$a_{45}=k_1A'A_{55}^s\alpha^2+k_2B'A_{44}^s\beta^2+R\left(k_1A'\alpha^2+k_2B'\beta^2\right)-E_{11}^T\alpha^2-E_{22}^T\beta^2\ a_{55}=-\left(A_{55}^s\alpha^2+A_{44}^s\beta^2+F_{11}^T\alpha^2+F_{22}^T\beta^2+R^s\right)$$

$$M_{11}=-I_0,\quad M_{13}=\alpha I_1,\quad M_{14}=-k_1A'\alpha J_1,\ M_{15}=0$$

$$M_{22}=-I_0,\ M_{23}=\beta I_1,\quad M_{24}=-k_2B'\ \beta J_1,\ M_{25}=0$$

$$M_{33}=-I_0-I_2(\alpha^2+\beta^2),\quad M_{34}=J_2\left(k_1A'\alpha^2+k_2B'\beta^2\right),\ M_{35}=-J_2$$

$$M_{44}=-K_2\left(\left(k_1A'\right)^2\alpha^2+\left(k_2B'\right)^2\beta^2\right),\ M_{45}=M_{35}\ M_{55}=-K_3$$